Available online at www.sciencedirect.com

ScienceDirect

Current Opinion in Electrochemistry

Review Article

Modeling electrochemical interfaces from ab initio molecular dynamics: water adsorption on metal surfaces at potential of zero charge

Jia-Bo Le and Jun Cheng

Abstract

The origin of the potential difference between the potential of zero charge of a metal/water interface and the work function of the metal is a recurring issue because it is related to how water interacts with metal surface in the absence of surface charge. Recently ab initio molecular dynamics method has been used to model electrochemical interfaces to study interfacial potential and the structure of interface water. Here, we will first introduce the computational standard hydrogen electrode method, which allows for ab initio determination of electrode potentials that can be directly compared with experiment. Then, we will review the recent progress from ab initio molecular dynamics simulation in understanding the interaction between water and metal and its impact on interfacial potential. Finally, we will give our perspective for future development of ab initio computational electrochemistry.

Addresses

State Key Laboratory of Physical Chemistry of Solid Surfaces, IChEM, College of Chemistry and Chemical Engineering, Xiamen University, Xiamen, 361005, China

Corresponding author: Cheng, Jun (chengjun@xmu.edu.cn)

Current Opinion in Electrochemistry 2020, **19**:129–136

This review comes from a themed issue on **Fundamental and Theoretical Electrochemistry**

Edited by **Galina Tsirlina**

For a complete overview see the Issue and the Editorial

Available online 9 December 2019

https://doi.org/10.1016/j.coelec.2019.11.008

Keywords

Metal–water interfaces, Potential of zero charge, ab initio molecular dynamics, Computational standard hydrogen electrode, Water chemisorption.

Introduction

The water molecules at electrochemical metal–water interfaces not just serve as the solvation medium but also can be reactants for many electrocatalytic reactions, for example, hydrogen evolution reaction [1] and oxygen reduction reaction [2,3]. Therefore, understanding the structure of the adsorbed water at the interface and its interaction with metal surface are of close relevance to electrocatalysis. The study of the electrochemical interfaces normally starts from the condition of potential of zero charge (PZC) [4,5], which is defined as the potential at which there is no charge on the electrode surface. The Gouy-Chapman theory predicts that the PZC corresponds to the minimum of the differential capacity in a dilute solution, which has been successfully used to determine the PZC for various metal electrodes such as Ag and Au [6]. However, this approach is often not suitable for platinum group metals because of the presence of surface adsorbates. Thus, two different definitions of PZC are proposed [7,8], namely, potential of zero total charge (PZTC) and potential of zero free charge (PZFC). The PZTC is the potential at which the sum of the surface free charge and the charge transferred upon adsorption equals zero. When there is no specific adsorption, the PZTC coincides with the PZFC, and only in this case it is an intrinsic property of the interface. Significant efforts have been made in literature to distinguish these two and determine the PZFC, see for example, the recent work on Pt from Rizo et al. [5]. Computation has certain advantage of modeling pristine interfaces, and thus in this work we only consider the PZC in the absence of specific adsorption.

Elucidating the interfaces at PZC helps to reveal how water interacts with metal surfaces, chemically or physically, in the absence of electric field, serving as good reference for the structure of interface water when a bias is applied. As shown in Figure 1a, the PZC of a metal–water interface (U_{PZC}) is related to the work function of its metal surface (Φ_M) [9],

$$e_0 U_{PZC} = \Phi_M - \Phi_{SHE} + \Delta\Phi. \quad (1)$$

The Φ_{SHE} in Eq. (1) denotes the absolute potential energy of the standard hydrogen electrode (SHE), which brings the U_{PZC} measured from an electrochemical cell in the same energy level of the Φ_M measured in vacuum. Note that there is an uncertainty in Φ_M from different measurements (4.28∼4.85 eV) [10–13], and we will take the value 4.44 eV as recommended by International Union of Pure and Applied

Figure 1

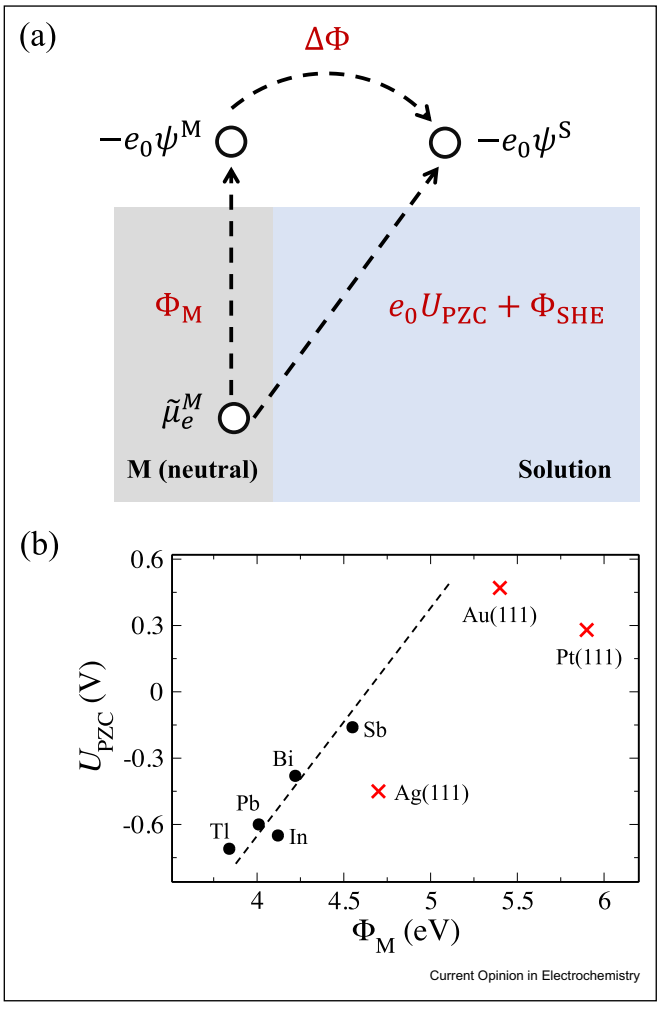

Relation between work function and potential of zero charge for metals. **(a)** Diagram for visualizing the definitions of the work function (Φ_M) of a metal surface and the potential of zero charge (PZC) ($e_0U_{PZC} + \Phi_{SHE}$) of a metal–water interface on the absolute scale. The $\Delta\Phi$ denotes the difference in the outer potential between the metal and solution phase (adapted from a study by Cheng [14]). **(b)** The PZC (U_{PZC}) on the SHE scale versus work function (Φ_M) for a series of metal–water interfaces. The data of the *sp* metal (Tl, In, Bi, Pb, and Sb) denoted by filled circles are fitted with Eq. (1), see the dashed line, and the data for three typical transition metal surfaces, that is, Pt(111), Ag(111) and Au(111), are represented with red cross marks (adapted from studies by Trasatti [6], Schmickler [9] and Le [15]).

Chemistry (IUPAC) for discussion in this work. The term $\Delta\Phi$ represents the difference in the outer (Volta) potential between metal and electrolyte solution (i.e. the potential at vacuum just outside the phase). As seen in Figure 1b, the $\Delta\Phi$ is almost a constant (~ -0.2 eV) for *sp* metals [9]. However, the transition metal surfaces are significantly off the trend line, and the $\Delta\Phi$ value can be as large as $\sim$-1 eV for Pt(111).

For the sake of theoretical understanding, the $\Delta\Phi$ is often divided into two parts:

$$\Delta\Phi = \Delta\Phi_{ori} + \Delta\Phi_{el}. \quad (2)$$

The term $\Delta\Phi_{ori}$ in Eq. (2) denotes the potential change because of orientation of interfacial water, and the $\Delta\Phi_{el}$ is because of electronic redistribution upon water adsorption. Although it is not obvious, if possible, to separate these two terms, $\Delta\Phi_{ori}$ and $\Delta\Phi_{el}$. As such, the large deviation in $\Delta\Phi$ for Pt(111) [16] and other transition metals is not well understood. Recently, development in computational work has provided new insight into this issue [15,17,18]. In particular, the ab initio molecular dynamics (AIMDs) method not only treats the dynamic behavior of liquid electrolyte solution but also correctly captures the electronic structure of metal electrode and the electronic interaction between metal and water, thus faithfully describing both the structure and electronic structure of the electrochemical interface [15,19,20].

Here, we will briefly review the recent progress in AIMD simulations of the metal–water interface at PZC. First, we will introduce the computational standard hydrogen electrode (cSHE) method, for calculating the electrode potential of the metal–water interface for comparison with experiment. Then, we will describe the structure of the interfacial water at PZC from AIMD and show that the chemical interaction between water and metal surface can induce a dramatic potential change at the interface. At last, we present an outlook on the necessity for developing other computational reference electrodes and the significance in understanding the role of the chemisorbed water in the presence of the electric double layer (EDL).

cSHE method

Based on the definitions aforementioned [5], the atomistic model of an electrochemical interface built by simply merging a metal surface and water film in a periodic cell corresponds to the condition of PZTC in the absence of surface adsorbates (i.e. PZFC). The model is then used for AIMD simulation for equilibration and configurational sampling. AIMD is a powerful tool for modeling electrochemical interfaces; and however, owing to the limitations in density functional, model size and time scale, the interface structures obtained from AIMD simulations are often subjected to criticisms that how realistic they are in comparison with experiment. Thus, it is very important to validate AIMD simulations by comparing physical properties that can be computed against their values that can be measured reliably by experiment. Among many others, PZC is probably one of the best physical quantities for benchmarking because PZC of many metal electrodes have been measured at high accuracy. On the other hand, there has been recent development for computing electrode potentials using AIMD. Most of computational work have adopted work function method in

which electrode potentials are calculated with reference to vacuum potential [21–24] and then converted into common electrochemical scale by subtracting the absolute potential of a reference electrode, for example, Φ_{SHE}, to compare with electrochemical measurements. However, the uncertainty in experimental Φ_{SHE}, as well as possible errors in treating the water–vacuum interface, incur some concern on the accuracy in the work function method.

In the following paragraph, we will introduce a different approach, that is, the cSHE method developed by Cheng [14,25,26] and Le [15]. The calculated electrode potentials using this method are directly comparable with experimental measurements without the need of resorting to estimated Φ_{SHE} and treating water–vacuum interface, thus unaffected by the uncertainty in Φ_{SHE} and surface potential of water. In the cSHE method, the half reaction of SHE ($H^+(aq) + e^-(vac) \rightarrow \frac{1}{2}H_2(g)$) is broken down into two parts, namely desolvation of aqueous proton ($H^+(aq) \rightarrow H^+(g)$) and reduction of H^+ into H_2 in the gas phase ($H^+(g) + e^-(vac) \rightarrow \frac{1}{2}H_2$ (g)). The latter is a gas phase reaction and the free energy can be readily obtained. For the former step, the free energy is calculated by deprotonation of aqueous H_3O^+ in periodic boxes (Figure 2a), which is the key in the cSHE method serving as internal potential reference under periodic boundary conditions. Thus, the electrode potential with respect to SHE can be calculated by referencing the Fermi level to the sum of the above two energies:

$$e_0U = -\varepsilon_F^{(i)} + \left(\Delta_{dp}A^{(i)}_{H_3O^+} - \Delta_f G^{g,o}_{H^+} - \Delta E_{ZP}\right). \quad (3)$$

The $\varepsilon_F^{(i)}$ and $\Delta_{dp}A^{(i)}_{H_3O^+}$ in Eq. (3) denote the Fermi level of a metal electrode and the deprotonation free energy of aqueous H_3O^+, as calculated in the same interface model (indicated by the superscript [*i*]), respectively. The $\Delta_f G^{g,o}_{H^+}$ represents the formation free energy of a gas-phase proton, that is, the energy of the reverse of the reaction $H^+(g) + e^-(vac) \rightarrow \frac{1}{2}H_2$ (g), and the ΔE_{ZP} is the zero-point energy correction for one O–H bond in the H_3O^+ missed in the calculation of $\Delta_{dp}A^{(i)}_{H_3O^+}$. Note that neither the calculated $\varepsilon_F^{(i)}$ nor $\Delta_{dp}A^{(i)}_{H_3O^+}$ alone has physical meaning due to an artificial offset in potential reference under periodic boundary conditions. Because both are calculated in the same interface model, their offsets are the same and canceled when combined in Eq. (3), giving rise to the physical potential *vs* SHE.

In the cSHE method, calculation of $\Delta_{dp}A^{(i)}_{H_3O^+}$ is very time-consuming because this free energy needs to be obtained by expensive thermodynamic integration scheme [26], which significantly limits its application to complex systems. Therefore, we further develop the cSHE method for the purpose of increasing its efficiency [15]. As shown in Figure 2, the interface model is coupled with a pure water model in the new scheme, and then the term $\Delta_{dp}A^{(i)}_{H_3O^+}$ in Eq. (3) can be replaced by the deprotonation energy of a H_3O^+ in the pure water model ($\Delta_{dp}A^{(w)}_{H_3O^+}$) with the adjustment of the electrostatic potential energy difference of bulk water between these two models ($e_0\phi^{(w)}_{wat} - e_0\phi^{(i)}_{wat}$). Note that the $e_0\phi^{(w)}_{wat}$ in pure water box must be zero in Ewald summation. Thus, the electrode potential can be reformulated as

$$e_0U = -\varepsilon_F^{(i)} + \left(\Delta_{dp}A^{(w)}_{H_3O^+} - e_0\phi^{(i)}_{wat} - \Delta_f G^{g,o}_{H^+} - \Delta E_{ZP}\right). \quad (4)$$

Comparing with the former version of the cSHE, this new scheme increases the efficiency of electrode potential calculation by a factor of ~10. Furthermore, its accuracy has been validated by computing the PZC of various metal/water interfaces, for example, Pt(111), Ag(111) and Au(111), and all of the calculated PZC are within the error of 0.1 V comparing with the experimental estimates [5,15,27]. This positive agreement also suggests that the AIMD simulations are sufficient to converge the interface potentials at relevant timescale and thus give reasonable representative structures of the interfaces.

Water adsorption on metal surfaces at PZCs

In this section, we will review the recent progress in studying the structures of metal/water interfaces using AIMD. As shown in Figure 3, we will mainly take the Pt(111)/water interface as an example to elucidate how water is adsorbed on transition metal surface at PZC. Early literature proposed the so-called ice-like bilayer structure of water at electrochemical interfaces, which was often used to model the solvent environment in computational electrocatalysis [29,30]. The ice-like bilayer structure originated from low-energy electron diffraction patterns [31] and scanning tunneling microscopy images [32] observed in ultrahigh vacuum (UHV) conditions and was also supported by density functional theory calculations [33]. However, owing to such great difference between electrochemical condition and UHV, it is quite dubious to assume the bilayer structure at electrochemical interfaces. Later, it was reported that the ice-like bilayer structure of water is actually not stable on Pt(111) and other transition metal surfaces using AIMD simulation [34–37].

Figure 3a shows a representative configuration of adsorbed water at the Pt(111)–water interface at PZC from AIMD simulation, showing no sign of ordered patterns of surface water. Further analysis reveals that part of the surface water is chemisorbed on Pt(111), that is, the water (named watA) highlighted with blue in Figure 3a, corresponding to the first peak of the water

Figure 2

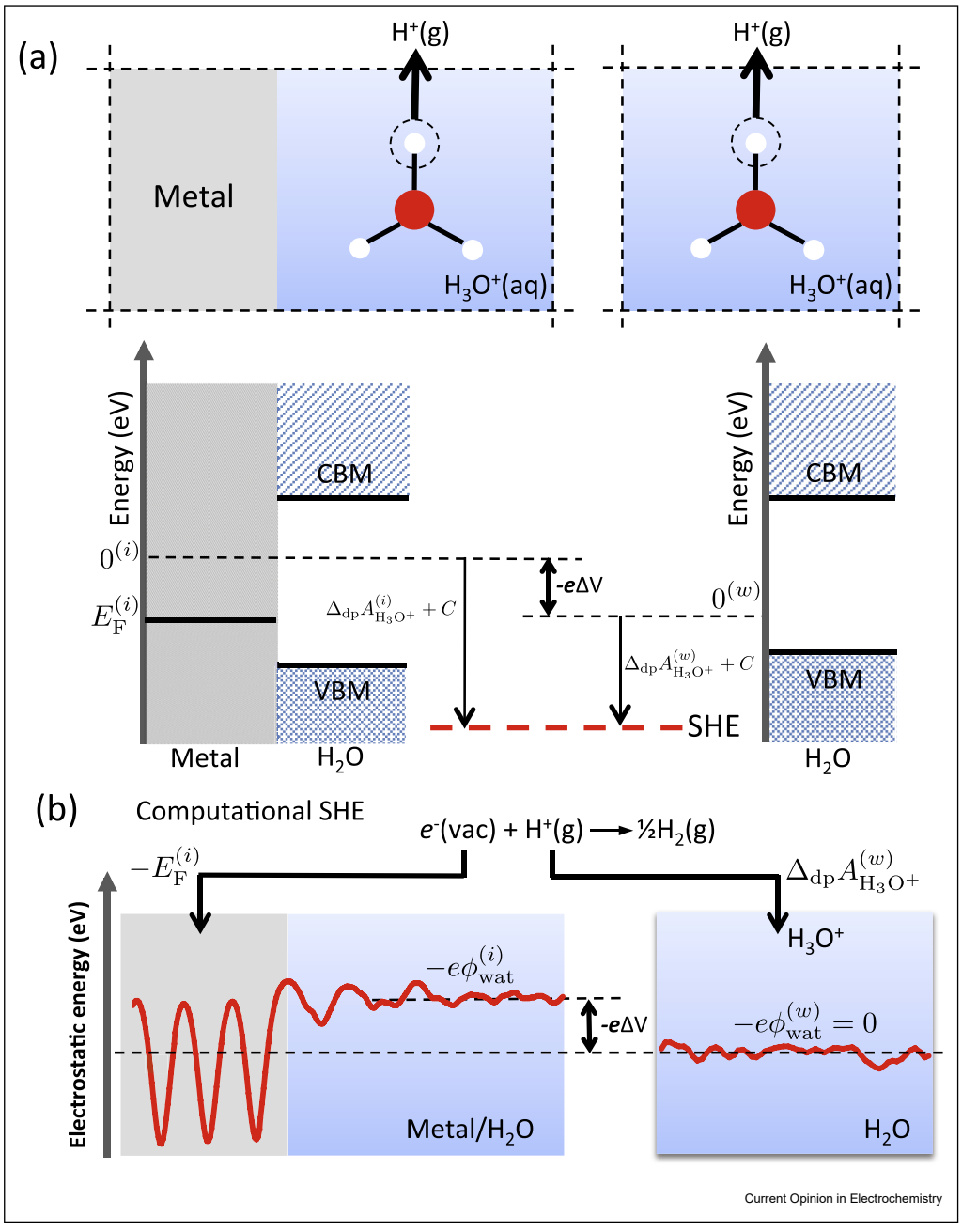

Scheme of the computational standard hydrogen electrode method [15]. (a) Two models are used in the scheme, namely, a metal–water interface model and a pure water model. Owing to the difference of the Hartree potential shifts in the two models, the computed deprotonation free energy of aqueous hydronium in the interface model differs from that in pure water model by e0V. (b) The difference between the computed electrostatic potentials of the water phase in the two models equals to e0V, and thus, $\Delta_{dp}A^{(i)}_{H_3O^+} - \Delta_{dp}A^{(w)}_{H_3O^+} = -e_0\phi^{(i)}_{wat} - (-e_0\phi^{(w)}_{wat})$.

density ρ_{H_2O} distribution in Figure 3b [15,34]. The structure of the chemisorbed water at Pt(111)–water interface is very similar to the configuration of a water monomer on Pt(111) in vacuum as reported in literature [38], sitting on the top site of the surface and with its molecular plane nearly paralleled with the surface. This configuration benefits from large hybridization between the $1b_1$ orbital of water and the *d* orbital of Pt, favoring formation of the chemical bond. Note that the chemisorbed water is generally found on other transition metal surfaces, for example, Au(111) and Ag(111) [15,34]. Furthermore, it should be pointed out that the choice of the density functional can affect the structure distribution of surface water. Comparing the results in

Figure 3

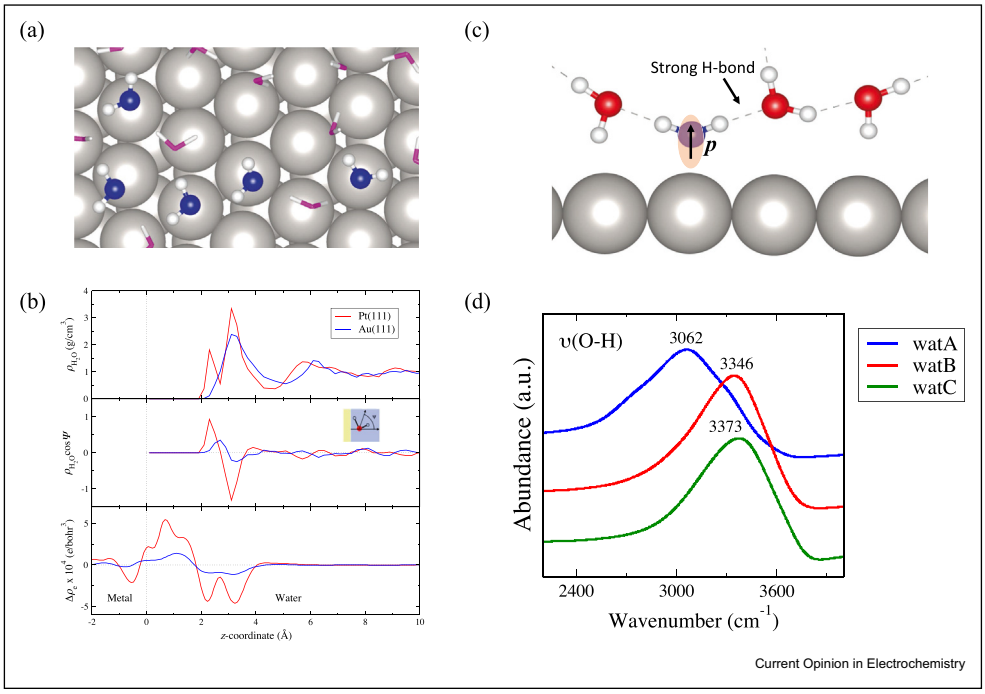

Properties of the chemisorbed water on metal surfaces. **(a)** Representative snapshot of the adsorbed water layer on Pt(111) at PZC. The Pt atoms, chemisorbed water, and some other interface water are colored in gray, blue, and pink (adapted from a study by Le et al. [28]). **(b)** Water density (ρ_{H_2O}), water dipole orientation ($\rho_{H_2O}\cos\Psi$), and electron density difference ($\Delta\rho_e$) distribution at the Pt(111)/water and Au(111)/water interface along the surface normal direction (*z*-coordinate) ([15]). **(c)** Proposed model for the structure of the adsorbed water layer on transition metal surfaces at PZC. The *p* indicates the dipole of the surface water induced by chemisorption (adapted from a study by Le et al. [28]). **(d)** Calculated vibrational density of states of the O–H stretching mode of watA (blue), watB (red), and watC (green) at the Pt(111)/water interface. See the main text for definitions of watA, watB and watC (adapted from a study by Le et al. [28]). PZC, potential of zero charge.

literature, we note that the peak ($z < 2.8$ Å) for the chemisorbed water obtained with Perdew-Burke-Ernzerhof functional with Grimme D3 correction (PBE-D3), as shown in Figure 3b, is not shown in the calculation with revised Perdew-Burke-Ernzerhof functional with Grimme D3 correction (RPBE-D3) [21]. In view that the computed PZC and $\Delta\Phi$ with RPBE-D3 functional are less accurate, we regard that the PBE-D3 functional has a better performance than the RPBE-D3 in modeling the Pt(111)–water interface.

As seen in Figure 3b, water chemisorption results in significant electron redistribution at the interface, which was also found in other publications [17–19]. It was reported that the electron redistribution can lead to the interfacial potential change $\Delta\Phi_{el}$ by −1.3 and −0.5 eV for the Pt(111)–water interface and Au(111)–water interface, respectively [15]. Combining Eqs. (1) and (2), we can reach an interesting conclusion that the $\Delta\Phi$ of metal–water interfaces at PZC is dominated by $\Delta\Phi_{el}$. Furthermore, from Figure 3b, $\Delta\Phi_{el}$ greatly depends on the binding between chemisorbed water and metal surface. Thus, the strong overlap with d band in transition metals like Pt can explain the deviation from the trend line of *sp* metals as shown in Fig. 1(b).

On the basis of the AIMD trajectories, we propose a simple model for the structure of the transition metal–water interfaces [34]. As can be seen from Figure 3c, apart from the watA, other surface water molecules (named watB) are composed of two main types of configurations, that is, 'H-up' and 'H-down'. It is interesting that the calculated orientational dipole ($\rho_{H_2O}\cos\Psi$) of the watB almost completely cancels the orientational dipole of watA (Figure 3b). Therefore, the overall orientational dipole of the interfacial water (Φ_{ori}) is very small, leading to negligible contribution to $\Delta\Phi$ at the transition metal–water interfaces [15].

Figure 3c also indicates the hydrogen bond network within the surface water layer and on Pt(111), the hydrogen bonds formed around watA appear stronger than those in bulk water because the distance between the two O atoms (d_{O-O}) is shorter than that in bulk water [28]. In experiment, the information of water hydrogen bonding is mostly extracted from vibrational spectra [39–41], and thus the vibrational frequencies of the water at interface were analyzed by calculating the vibrational density of states [28,40,42]. As can be seen in Figure 3d, the calculated stretching frequency of O–H bonds of watA ($\sim$3000 cm^{-1}, a similar peak has been

observed in infrared (IR) experiments [41]) has an apparent red-shift comparing with bulk water, also consistent with the observation that the d_{O-O} around watA is shorter than that in bulk water [43]. The formation of the strong hydrogen bonds can be explained by the fact that watA is chemisorbed on the Pt(111) surface, leading to electron deficiency in watA and thus strong attraction to the O atoms of neighboring water.

Outlook

AIMD has unique advantages for simulating electrochemical interfaces and can complement the existing experimental techniques for understanding the microscopic properties of the interfaces. AIMD simulations of electrochemical interfaces at PZC have shown that there exists chemisorbed water at the interfaces, and thus interfacial charge redistribution, which can lead to significant interfacial potential shift and formation of strong hydrogen bonds with adjacent water. Note that it is well known in surface science that water can chemically adsorb on transition metals in vacuum; whereas its implication in the context of interfacial electrochemistry is somewhat less explored. Because water chemisorption has significant impact on interfacial potential, one would expect that they may also affect the dielectric properties of EDL and hence the electrocatalytic reactions (e.g. oxygen reduction reaction and hydrogen evolution reaction) occurring in EDL. These investigations, although expensive, should now be within the reach of AIMD. To further explore these with AIMD, the challenge is how to model realistic EDL at electrochemical interfaces. Despite some recent progress [40,44—46], the microscopic structure and capacitive behavior of EDL are far from being understood.

We stress that it is important to determine the electrode potential of a simulated electrochemical interface because it demonstrates the relevance of the model to experiment. The developed cSHE method works well for aqueous electrochemistry but many electrochemical systems including energy storage and conversion devices, involve nonaqueous electrolyte solutions such as organic solvents and room temperature ionic liquids. Appropriate reference electrodes should be used for the specific electrochemical conditions [47], for example, Ag/AgCl reference electrode [48] and some quasi-reference electrodes. Thus, the computational reference electrode approach should be further developed for nonaqueous systems.

The high computational cost of AIMD will significantly limit its application to more complex electrochemical systems. One would have to resort to multiscale methods such as quantum mechanics/molecular mechanics (QM/MM) [49] and continuum models [50]. It is important to bear in mind that AIMD can serve very good benchmarks for developing these methods. It can help at least in two scenarios: (i) physical understanding obtained from AIMD can help make appropriate approximations or simplifications wherever possible and (ii) some physical interactions that are found to be important in AIMD will need to be preserved in the multiscale methods so that key factors will not get missed. An obvious example for the latter is the chemisorption effect of water on electrode surfaces. Finally, the recent surge of machine learning—based potentials has been gradually changing the landscape of molecular and materials modeling [51—54]. The significant speed-up of 1000—10000 times comparing with density functional theory is very appealing for simulating electrochemical systems. There is however long way to go because it is not yet clear how to systematically incorporate the long-range electrostatic interaction and charge states of electrodes and ions in the machine learning—based potentials.

Conflict of interest statement

Nothing declared.

Acknowledgements

This work is supported by the National Natural Science Foundation of China (Grants No. 21861132015, 21621091 and 21902136) and the China Postdoctoral Science Foundation (2018M642563).

References

Papers of particular interest, published within the period of review, have been highlighted as:

* of special interest
** of outstanding interest

1. Ledezma-Yanez I, Wallace WDZ, Sebastián-Pascual P, Climent V, Feliu JM, Koper MTM: **Interfacial water reorganization as a pH-dependent descriptor of the hydrogen evolution rate on platinum electrodes**. *Nat Energy* 2017, **2**:17031.

2. Dong JC, Zhang XG, Briega-Martos V, Jin X, Yang J, Chen S, Yang ZL, Wu DY, Feliu JM, Williams CT, Tian ZQ, Li JF: **In situ Raman spectroscopic evidence for oxygen reduction reaction intermediates at platinum single-crystal surfaces**. *Nat Energy* 2019, **4**:60.

3. Kulkarni A, Siahrostami S, Patel A, Nørskov JK: **Understanding catalytic activity trends in the oxygen reduction reaction**. *Chem Rev* 2018, **118**:2302.

4. Huang J, Zhou T, Zhang J, Eikerling M: **Double layer of platinum electrodes: non-monotonic surface charging phenomena and negative double layer capacitance**. *J Chem Phys* 2018, **148**. 044704.

5. Rizo R, Sitta E, Herrero E, Climent V, Feliu JM: **Towards the understanding of the interfacial pH scale at Pt(111) electrodes**. *Electrochim Acta* 2015, **162**:138.

6. Trasatti S: **Work function, electronegativity, and electrochemical behaviour of metals: II. Potentials of zero charge and "electrochemical" work functions**. *J Electroanal Chem Interfacial Electrochem* 1971, **33**:351.

7. Frumkin A, Petrii O: **Potentials of zero total and zero free charge of platinum group metals**. *Electrochim Acta* 1975, **20**:347.

8. Petrii OA: **Zero charge potentials of platinum metals and electron work functions (Review)**. *Russ J Electrochem* 2013, **49**:401.

9. Schmickler W: **Electronic effects in the electric double layer**. *Chem Rev* 1996, **96**:3177.

10. Tripkovic V, Björketun ME, Skúlason E, Rossmeisl J: **Standard hydrogen electrode and potential of zero charge in density functional calculations**. *Phys Rev B* 2011, **84**:115452.

11. Trasatti S: **The absolute electrode potential: an explanatory note (Recommendations 1986)**. *Pure Appl Chem* 1986, **58**:955.

12. Isse AA, Gennaro A: **Absolute potential of the standard hydrogen electrode and the problem of interconversion of potentials in different solvents**. *J Phys Chem B* 2010, **114**: 7894.

13. Fawcett WR: **The ionic work function and its role in estimating absolute electrode potentials**. *Langmuir* 2008, **24**:9868.

14. ** Cheng J, Sprik M: **Alignment of electronic energy levels at electrochemical interfaces**. *Phys Chem Chem Phys* 2012, **14**: 11245.

This paper reviewed the theory of electrochemical potentials and summarized the general methods for computing level alignment at electrochemical interfaces.

15. ** Le J, Iannuzzi M, Cuesta A, Cheng J: **Determining potentials of zero charge of metal electrodes versus the standard hydrogen electrode from based on density-functional-theory-based molecular dynamics**. *Phys Rev Lett* 2017, **119**. 016801.

This paper reported the latest development of the cSHE method, and showed that charge redistribution due to water chemisorption can lead to dramatic potential changes at transition metal/water interfaces.

16. Cuesta A: **Measurement of the surface charge density of CO-saturated Pt(111) electrodes as a function of potential: the potential of zero charge of Pt(111)**. *Surf Sci* 2004, **572**:11.

17. * Jinnouchi R, Anderson AB: **Electronic structure calculations of liquid-solid interfaces: combination of density functional theory and modified Poisson-Boltzmann theory**. *Phys Rev B* 2008, **77**:245417.

This paper showed the importance of explicit water on metal surfaces for calculating electrode potentials.

18. Yoon Y, Rousseau R, Weber RS, Mei D, Lercher JA: **First-principles study of phenol hydrogenation on pt and ni catalysts in aqueous phase**. *J Am Chem Soc* 2014, **136**:10287.

19. * Sakong S, Groß A: **The electric double layer at metal-water interfaces revisited based on a charge polarization scheme**. *J Chem Phys* 2018, **149**. 084705.

This paper also showed that the interfacial water has partial charge transfer to Pt(111) surface by using a charge population scheme.

20. Bouzid A, Pasquarello A: **Atomic-scale simulation of electrochemical processes at electrode/water interfaces under referenced bias potential**. *J Phys Chem Lett* 2018, **9**:1880.

21. Sakong S, Forster-Tonigold K, Groß A: **The structure of water at a Pt(111) electrode and the potential of zero charge studied from first principles**. *J Chem Phys* 2016, **144**:194701.

22. Taylor CD, Wasileski SA, Filhol J-S, Neurock M: **First principles reaction modeling of the electrochemical interface: consideration and calculation of a tunable surface potential from atomic and electronic structure**. *Phys Rev B* 2006, **73**:165402.

23. Otani M, Hamada I, Sugino O, Morikawa Y, Okamoto Y, Ikeshoji T: **Structure of the water/platinum interface - a first principles simulation under bias potential**. *Phys Chem Chem Phys* 2008, **10**:3609.

24. Pham TA, Ping Y, Galli G: **Modelling heterogeneous interfaces for solar water splitting**. *Nat Mater* 2017, **16**:401.

25. Cheng J, Liu X, VandeVondele J, Sulpizi M, Sprik M: **Redox potentials and acidity constants from density functional theory based molecular dynamics**. *Acc Chem Res* 2014, **47**: 3522.

26. Cheng J, Sulpizi M, Sprik M: **Redox potentials and pKa for benzoquinone from density functional theory based molecular dynamics**. *J Chem Phys* 2009, **131**:154504.

27. Koper MTM, Ojha K, Arulmozhi N, Aranzales D: **Double layer of Pt(111)-aqueous electrolyte interface: potential of zero charge and anomalous Gouy-Chapman screening**. *Angew Chem Int Ed* 2019, https://doi.org/10.1002/anie.201911929.

28. Le J, Fan Q, Perez-Martinez L, Cuesta A, Cheng J: **Theoretical insight into the vibrational spectra of metal-water interfaces from density functional theory based molecular dynamics**. *Phys Chem Chem Phys* 2018, **20**:11554.

29. Rossmeisl J, Logadottir A, Nørskov J: **Electrolysis of water on (oxidized) metal surfaces**. *Chem Phys* 2005, **319**:178.

30. Tripković V, Skúlason E, Siahrostami S, Nørskov JK, Rossmeisl J: **The oxygen reduction reaction mechanism on Pt(111) from density functional theory calculations**. *Electrochim Acta* 2010, **55**:7975.

31. Thiel PA, Hoffmann FM, Weinberg WH: **Monolayer and multilayer adsorption of water on Ru(001)**. *J Chem Phys* 1981, **75**: 5556.

32. Morgenstern K, Nieminen J: **Intermolecular bond length of ice on Ag(111)**. *Phys Rev Lett* 2002, **88**. 066102.

33. Carrasco J, Hodgson A, Michaelides A: **A molecular perspective of water at metal interfaces**. *Nat Mater* 2012, **11**:667.

34. Le J, Cuesta A, Cheng J: **The structure of metal-water interface at the potential of zero charge from density functional theory-based molecular dynamics**. *J Electroanal Chem* 2018, **819**:87.

35. Kristoffersen HH, Vegge T, Hansen HA: **OH formation and H2adsorption at the liquid water-Pt(111) interface**. *Chem Sci* 2018, **9**:6912.

36. * Schnur S, Groß A: **Properties of metal-water interfaces studied from first principles**. *New J Phys* 2009, **11**:125003.

This paper showed the structures and vibrational frequencies of several metal/water interfaces from AIMD simulations.

37. Bellarosa L, García-Muelas R, Revilla-López G, López N: **Diversity at the water–metal interface: metal, water thickness, and confinement effects**. *ACS Cent Sci* 2016, **2**: 109.

38. * Michaelides A, Ranea VA, de Andres PL, King DA: **General model for water monomer adsorption on close-packed transition and noble metal surfaces**. *Phys Rev Lett* 2003, **90**: 216102.

This paper studied adsorption of water monomer on close-packed transition metal surfaces. It found that the water monomer is preferred to be adsorbed on the top site, and with its molecular plane almost paralleled to surface.

39. Tong Y, Lapointe F, Thamer M, Wolf M, Campen RK: **Hydrophobic water probed experimentally at the gold electrode/aqueous interface**. *Angew Chem Int Ed* 2017, **56**:4211.

40. Li C-Y, Le J-B, Wang Y-H, Chen S, Yang Z-L, Li J-F, Cheng J, Tian Z-Q: **In situ probing electrified interfacial water structures at atomically flat surfaces**. *Nat Mater* 2019, **18**:697.

41. Osawa M, Tsushima M, Mogami H, Samjeské G, Yamakata A: **Structure of water at the electrified platinum-water interface: a study by surface-enhanced infrared absorption spectroscopy**. *J Phys Chem C* 2008, **112**:4248.

42. Lin X, Evers F, Groß A: **First-principles study of the structure of water layers on flat and stepped Pb electrodes**. *Beilstein J Nanotechnol* 2016, **7**:533.

43. Feibelman PJ: **What the stretch frequency spectrum of D2O/Ru(0001) does and does not mean**. *Chem Phys Lett* 2004, **389**: 92.

44. Groß A, Sakong S: **Modelling the electric double layer at electrode-electrolyte interfaces**. *Curr Opin Electrochem* 2018, **14**:1.

45. Cheng T, Wang L, Merinov BV, Goddard WA: **Explanation of dramatic pH-dependence of hydrogen binding on noble metal electrode: greatly weakened water adsorption at high pH**. *J Am Chem Soc* 2018, **140**:7787.

46. Sundararaman R, Figueiredo MC, Koper MTM, Schwarz KA: **Electrochemical capacitance of CO-terminated Pt(111) dominated by the CO–solvent gap**. *J Phys Chem Lett* 2017, **8**: 5344.

47. Gritzner G, Kůta J: **Recommendations on reporting electrode potentials in nonaqueous solvents: IUPC commission on electrochemistry**. *Electrochim Acta* 1984, **29**:869.

48. Yang X-H, Cuesta A, Cheng J: **A computational Ag/AgCl reference electrode from density functional theory-based molecular dynamics**. *J Phys Chem B* 2019, https://doi.org/10.1021/acs.jpcb.9b06650.

49. Bruix A, Margraf JT, Andersen M, Reuter K: **First-principles-based multiscale modelling of heterogeneous catalysis**. *Nat Catal* 2019, **2**:659.

50. Fisicaro G, Genovese L, Andreussi O, Marzari N, Goedecker S: **A generalized Poisson and Poisson-Boltzmann solver for electrostatic environments**. *J Chem Phys* 2016, **144**. 014103.

51. Zhang L, Han J, Wang H, Car R, Weinan E: **Deep potential molecular dynamics: a scalable model with the accuracy of quantum mechanics**. *Phys Rev Lett* 2018, **120**:143001.

52. Natarajan SK, Behler J: **Neural network molecular dynamics simulations of solid–liquid interfaces: water at low-index copper surfaces**. *Phys Chem Chem Phys* 2016, **18**:28704.

53. Huang J-X, Csányi G, Zhao J-B, Cheng J, Deringer VL: **First-principles study of alkali-metal intercalation in disordered carbon anode materials**. *J Mater Chem A* 2019, **7**:19070.

54. Bartók AP, Payne MC, Kondor R, Csányi G: **Gaussian approximation potentials: the accuracy of quantum mechanics, without the electrons**. *Phys Rev Lett* 2010, **104**:136403.